Analysis of a Rotating Spool Expander for Organic Rankine Cycles in Heat Recovery Applications

_____

International Compressor Engineering Conference at Purdue, July 14-17, 2014

Abhinav Krishna
Ray W. Herrick Laboratories
West Lafayette, Indiana

Craig R. Bradshaw, PhD
Torad Engineering LLC
Cumming, Georgia

Eckhard A. Groll, D.Sc.
Ray W. Herrick Laboratories
West Lafayette, Indiana

_____

Analysis of a Rotating Spool Expander for Organic Rankine Cycles in Heat Recovery Applications

Abhinav KRISHNA[1]*, Craig BRADSHAW[2], Eckhard GROLL[3]

[1] Purdue University, School of Mechanical Engineering
Ray W. Herrick Laboratories, West Lafayette, IN, 47907 USA
Fax – (765-494-0787), E mail – krishna1@purdue.edu

[2] Torad Engineering, 1005 Union Hill Road, Suite 2
Alpharetta, GA 30004
Phone – 678- 366- 3399, Fax – 678-366-3353, E mail – craig.bradshaw@toradengineering.com

[3] Purdue University, School of Mechanical Engineering
Ray W. Herrick Laboratories, West Lafayette, IN, 47907 USA
Fax – (765-494-0787), E mail – groll@purdue.edu

* Corresponding Author

ABSTRACT

A comprehensive simulation model of the rotating spool expander is presented. The simulation model includes detailed submodels for the geometry, suction valve mechanism, massflow, leakage and heat transfer processes. The results of the model reveal several details concerning the impact of design variables on performance. For example, the match between the design expansion ratio and the system imposed pressure ratio has a large influence on the performance of the expander. The reasons for this are analyzed, and further exploration shows that under-expansion is preferable to over-expansion to achieve better performance. The model is also able to provide insights on the dominant leakage paths in the expander. Additional insights can be obtained to assess the sensitivity of various design variables on expander performance. In future work, the model predictions will be validated using experimental data from a 50 kW prototype spool expander.

1. INTRODUCTION

The increasing cost of energy, coupled with the recent drive for energy security and climate change mitigation have provided the impetus for harnessing renewable energy sources as viable alternatives to conventional fossil fuels. Furthermore, recovering heat that is discharged from power plants, automobiles and various other industrial processes is of growing interest. However, technologies attempting to provide small-scale heat recovery solutions have seen very limited commercialization. This is broadly due to two reasons: lack of historical research and development in the area of waste-heat recovery and small-scale power generation due to technical and cost impediments; and technical challenges associated with scaling the technology from utility-scale to commercial-scale, particularly with regard to expansion machines (turbines). However, due to rising primary energy costs and the environmental premium being placed on fossil fuels, the conversion from low-grade heat to electrical energy as well as small-scale distributed power generation is of increasing interest. In this regard, this project focuses on a novel rotating spool expansion machine at the heart of an Organic Rankine Cycle (ORC), which in turn is applied as a heat recovery system.

The spool expander is similar to the spool compressor introduced by Kemp *et al.* (2008). The spool expander provides a new rotating expansion mechanism with easily manufactured components. Apart from efficiency improvements compared with other rotary machines, the spool expander also has the ability to control the expansion

ratio using a novel mechanically-driven suction valve mechanism. Another advantage is the relocation of the face sealing surfaces to the outer radius of the device. The spool expander is also scalable to a size range (50-200 kW) that is problematic for many conventional positive displacement machines (scrolls, pistons, etc.), and too small for dynamic machines with respect to manufacturability, efficiency and cost. A detailed geometry model of the spool expander and the suction valve mechanism is developed. This geometry model forms a part of a comprehensive model that includes submodels for massflow, leakage, and heat transfer. Given the promise of the technology, this paper explores the design space using a simulation based approach.

2. EXPANDER MODEL DESCRIPTION

The key components of the expander are shown in Figure 1 and Figure 2. The working principle is similar to a spool compressor operating in reverse:

- The vane is constrained by means of an eccentric cam allowing its distal end to be held in very close proximity to the expander housing while never contacting it. A tip seal closes the clearance gap between the vane and housing.
- The rotor is fixed to endplates that rotate with the central hub and vane, thus forming a rotating spool. A cam groove is machined into the end plates, which drives the suction valve.
- Dynamic seals are needed to isolate the various process pockets from each other as well as from the expander shell.
-
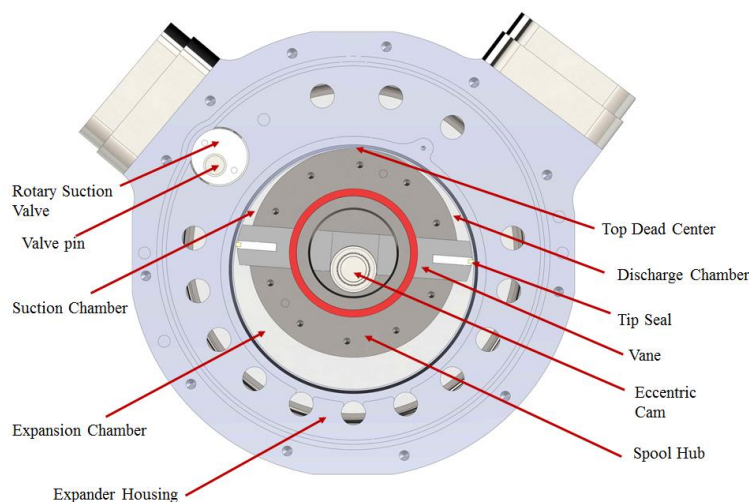
Figure 1: Cutaway rear view of the rotating spool expander showing key features.
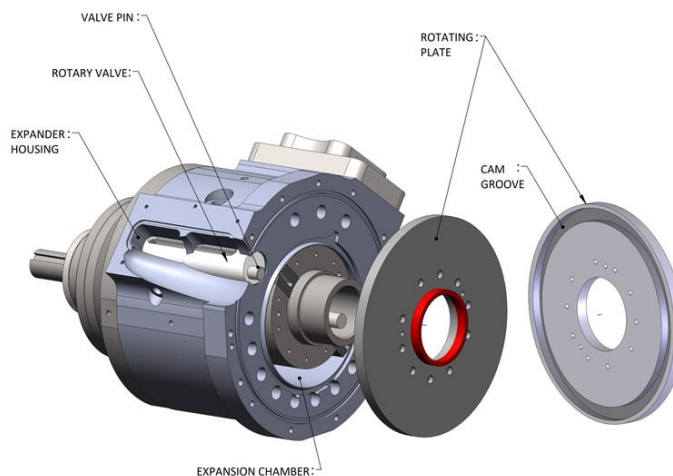

Figure 2: Partial assembly view of the rotating spool expander showing key features.

The model development follows the same approach as detailed in Bradshaw *et al.* (2013), Bell (2011), Mathison *et al.* (2008, 2011) for positive displacement compressors. Bradshaw *et al.* (2013) applied the comprehensive modeling approach to a rotating spool compressor. The expander model development is analogous to this, with several modifications listed below.
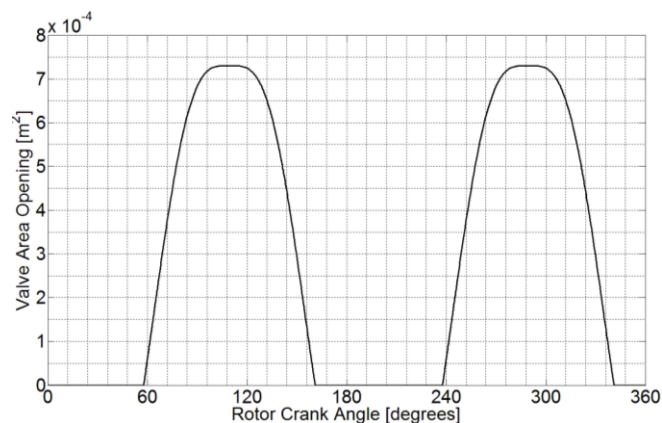
2.1 Suction Valve Model

The novel, cam-driven suction valve mechanism, shown in Figure 3, is unique to the rotating spool expander and provides the ability to control the expansion ratio of the machine. The working principle is as follows: the cam groove profile is machined into the rotating end plates of the expander. The cam groove drives an oscillating roller follower, which in this case is a pin/bushing that is part of the suction valve assembly. The movement of the pin causes the suction valve to rotate. The openings in the suction valve align with those bored into the expander housing in chosen proportions at various crank angles, allowing a prescribed amount of charge to enter the suction chamber of the expander.
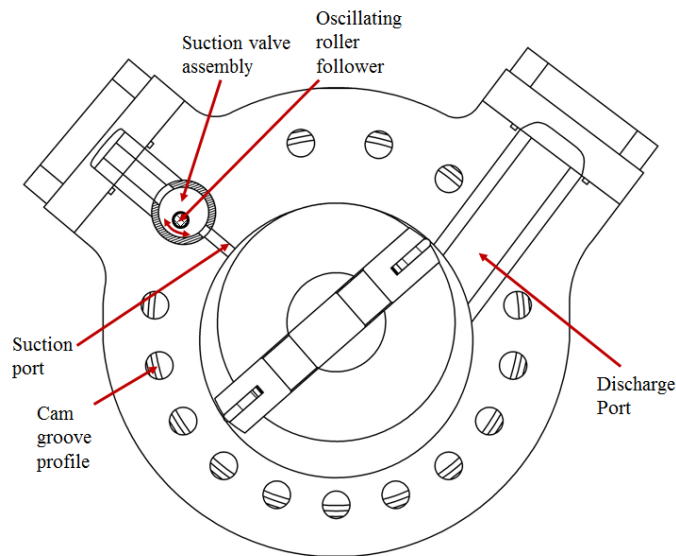
Figure 3: Simplified representation of suction valve mechanism.

This mechanism requires careful analysis of the cam profile and associated kinematics and dynamics of the system. In this regard, the analysis presented by Norton (2009) provides the framework to assess the performance of the cam-oscillator mechanism. A 4-5-6-7 polynomial cam profile is utilized because of the continuous acceleration and jerk profiles of the oscillating roller follower. Using the selected cam profile it is possible to analytically determine the co-ordinates of the cam surface profile and the path of the oscillating roller follower. Figure 4 shows the valve area opening as a function of crank angle that is the result of this analysis. Note that this area profile can be modified by manipulating the cam profile, which in turn can be used to modify the expansion ratio of the machine.

Figure 4: Valve area opening as a function of rotor crank angle for the suction valve mechanism.

Figure 5 shows the pressure angle of the oscillating roller follower as a function of crank angle. The pressure angle is an important design consideration in cam-follower systems because it directly influences friction, wear and ultimately the performance and integrity of the system. In general, pressure angles with absolute values below 30 degrees are necessary (Norton, 2009). As shown, the chosen design meets this requirement.
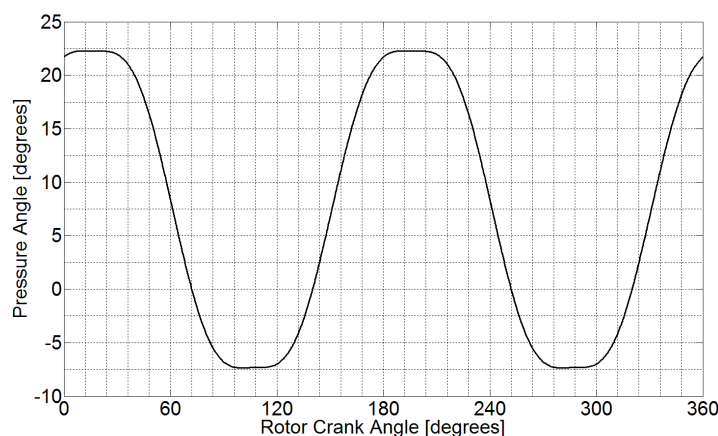

Figure 5: Pressure angle of cam on follower as a function of rotor crank angle for the suction valve mechanism.

2.2 Geometry of Chambers
The analytical expressions for the volumes of the suction and discharge chambers are identical to those given in Bradshaw et al. (2013) and will not be repeated here. The volume of the compression chamber in Bradshaw et al. (2013) is replaced with an identical expression for the expansion chamber in this model. Furthermore, the spool vane geometry and the associated tip seal are also identical.

2.3 Mass Flow and Leakage Models
A mass balance is developed for the charge within the suction, expansion and discharge chambers. The openings on the top of the suction valve are open to the suction pipe throughout as the valve oscillates, even when the openings at the bottom of the valve are closed to the suction chamber. Thus, the suction valve will always remain at high pressure. The mass into the suction chamber is controlled by the valve mechanism and the location of the vane. Before the vane passes the suction port, any charge present in the valve and suction port fills the expansion chamber. For the period when the vane tip seal is between the edges of the suction port, the charge is allocated to both the suction and expansion chambers based on the area opening of each chamber as shown in Figure 6. As the vane passes the trailing edge of the suction port, the charge fills the suction chamber. When the vane passes the 180º mark, the suction chamber and the charge within it transitions into the expansion chamber.
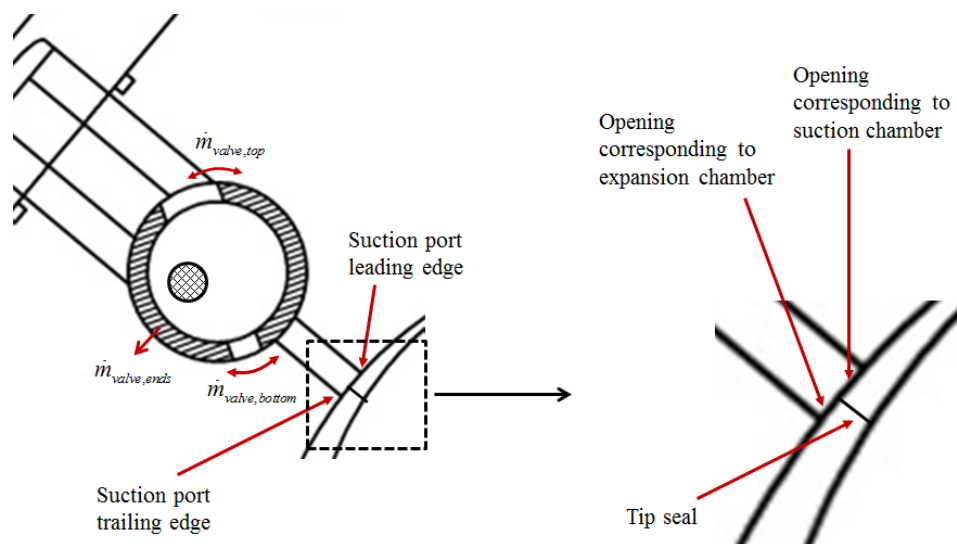
Figure 6: Representation of mass flow and leakage paths as the vane passes the suction valve port.

The mass flow out of the discharge chamber is analogous to that coming into the suction chamber. Before the vane passes the discharge port, any gas present in the discharge chamber is exposed to the discharge port and flows out of it. For the period when the vane is between the edges of the discharge port, the charge flows out of both the expansion and discharge chambers based on the area opening of each chamber. As the vane passes the trailing edge of the discharge port, only the expansion chamber is exposed to the discharge port and the charge flows out of this chamber. Note that any residual gas remaining in the discharge chamber after the vane has passed the trailing edge of the discharge port is recompressed and forced past the Top Dead Center (TDC).

The leakage paths in the spool expander are identical to those detailed for the spool compressor in Bradshaw *et al.* (2013). The relative pressures in each chamber, however, mean that the flow direction of any leaking fluid is likely to be different than for a compressor i.e. the suction chamber pressure is generally higher than the pressure in the expansion chamber, which in turn is higher than the discharge chamber pressure. There are also three additional leakage pathways due to the suction valve mechanism as shown in Figure 6: one emanating from the suction pipe and flowing around the valve into the suction chamber; another one that is located at the valve ends; a third one when the valve is partially or fully closed, leading directly into the suction chamber. Note, however, that the limiting gap in all of these cases is the clearance between the valve and expander housing.

Finally, once all of the possible flow paths are determined, a mass balance for each chamber can be written as (Bradshaw *et al.*, *2013*):

$$\frac{d\rho}{d\theta} = \frac{1}{V}\left[-\rho\frac{d\rho}{d\theta} + \frac{1}{\omega}\left(\sum \dot{m}_{in} - \sum \dot{m}_{out} \right) \right] \tag{1}$$

where ρ is the chamber density, V is chamber volume, θ is the rotor crank angle, ω is the rotational speed, $\dot{m}_{in}$ is the massflow into the chamber from all possible flow paths and $\dot{m}_{out}$ is the massflow out of the chamber from all possible flow paths. The above expression is evaluated for each crank angle increment.

2.4 Energy Balance
An energy balance to calculate the change in temperature in each chamber can be written as (Bradshaw *et al.*, *2013*):

$$\frac{dT}{d\theta} = \frac{-\rho h \frac{dV}{d\theta}\left[uV + \rho V \frac{\partial u}{\partial \rho} \right]\frac{\partial \rho}{\partial \theta} + \frac{1}{\omega}\left[\dot{Q} + \sum \dot{m}_{in} h_{in} - \sum \dot{m}_{out} h_{out} \right]}{\rho V \frac{\partial u}{\partial T}} \tag{2}$$

where T is the chamber temperature, ρ is the chamber density, u is the chamber internal energy, V is chamber volume, θ is the crank angle, ω is the rotational speed, $\dot{m}_{in}$ and $\dot{h}_{in}$ are the massflow and enthalpy, respectively, into the chamber from all possible flow paths, and $\dot{m}_{out}$ and $\dot{h}_{out}$ are the massflow and enthalpy, respectively, out of the chamber from all possible flow paths. The mass and energy balances are coupled, and two independent thermophysical properties need to be selected in order to fix the state at each control volume within the expander. For this project, temperature and density were chosen as the independent properties as shown in (1) and (2) due to the ease computing derivatives.

2.5 Heat Transfer Model
The heat transfer sub-model follows the approach by Mathison *et al.* (2008) and utilizes a spiral heat exchange model to calculate the convective heat transfer coefficient between the gas in each of the chambers and the cylinder wall:

$$h_c = 0.023 \frac{k}{D_h} \mathrm{Re}^{0.8} \mathrm{Pr}^{0.4} \left[1.0 + 1.77 \left(\frac{D_h}{r} \right) \right] \tag{3}$$

where the Reynolds number and the Prandtl number are calculated using gas properties in each of the chambers, D_h is the hydraulic diameter and r is the radius of the chamber. In addition, the modified Dittus-Boelter equation is used to calculate the heat transfer from the suction pipe to the expander shell:

$$h_c = 0.023 \frac{k}{D_h} \mathrm{Re}^{0.8} \mathrm{Pr}^{0.4} \tag{4}$$

Note that for these calculations, the temperature of the cylinder surface is initially unknown and solving for the heat transfer is therefore an iterative process. In addition, the radial distribution of cylinder temperature around the cylinder is unknown. Based on prior experience (Mathison *et al.*, 2011), a linear radial temperature distribution was assumed, varying from 5 K above the average cylinder temperature near the suction port to 5 K below the average cylinder temperature near the discharge port. Based on the temperatures in each chamber, a simple shell energy balance is applied to the expander estimate the temperature of the gas in the shell, and the heat loss to the ambient environment.

Finally, Figure 7 summarizes the procedure used for solving the entire numerical model.
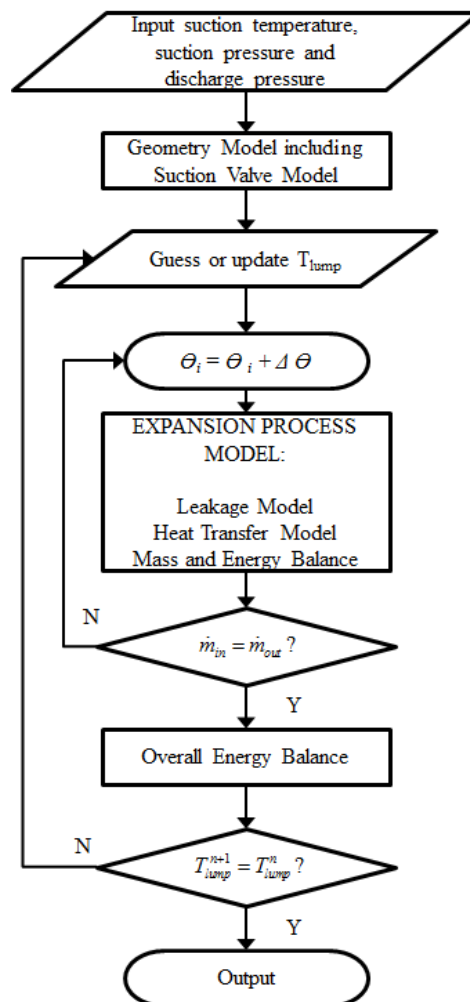

Figure 7: Flow chart showing the numerical procedure employed in a spool expander model.

3. RESULTS AND DISCUSSION

The comprehensive model provides a valuable tool to characterize the performance of the spool expander, and study the impact of various design variables to the performance of the machine. As an example, consider the expansion ratio as an independent design variable. Figure 8 shows a Pressure-Volume diagram for a spool expander designed for a 50kW output with an expansion ratio of 2.4. Holding all other parameters constant, Figure 9 and Figure 10 show the same expander operating in a system where the pressure ratio is 3.0 and 2.0 respectively.
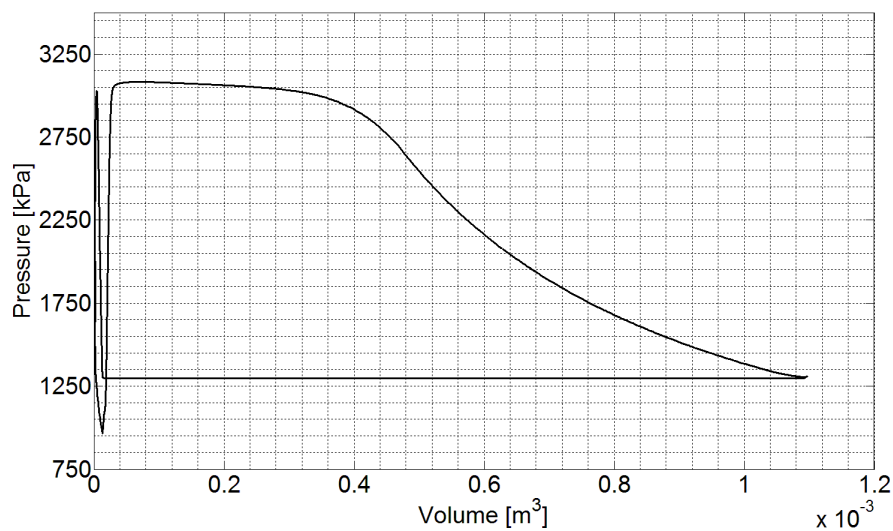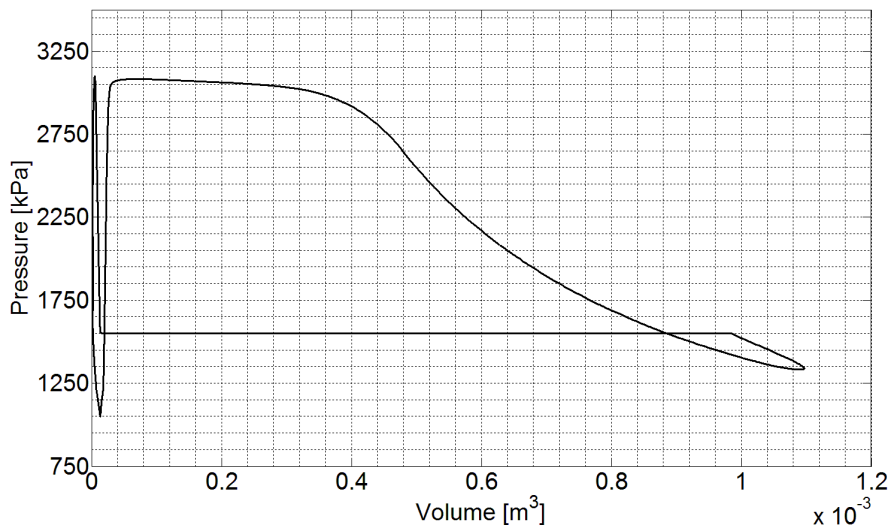
Figure 8: P-V diagram of expansion process at design conditions.
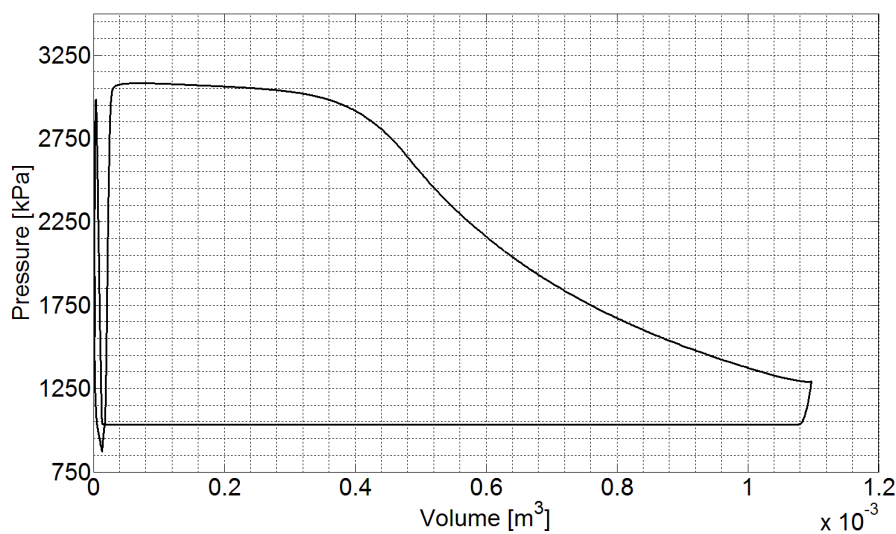
**Figure 9:** P-V diagram of expansion process for an under-expanded case.

Figure 10: P-V diagram of expansion process for an over-expanded case.

Figure 8 constitutes the perfectly expanded "base case" for the spool expander design. The sudden drop in pressure at the beginning of the cycle is due to the suction chamber pulling a partial vacuum until the vane tip passes the suction valve opening, and fresh charge begins to fill the suction chamber. Commensurately, the pressure spike at the end of the cycle is due to the fact that some residual charge is recompressed in the discharge chamber as the vane tip passes the trailing edge of the discharge port, and is forced past the TDC.

Figure 9 shows the under-expanded case since the system pressure ratio is larger than the design expansion ratio of the machine. A key difference when comparing this result to the base case is the sudden expansion of the charge at the end of the expansion process. Since the built-in geometry of the expander cannot expand the gas to a low enough pressure, as the vane tip passes the leading edge of the discharge port there is a sudden expansion process as the gas communicates with the line discharge pressure. This results in a loss of recoverable work, and correspondingly, a loss in power output.

Figure 10 shows the over-expanded case since the system pressure ratio is smaller than the design expansion ratio of the machine. In this case, the gas is expanded to a pressure lower than the line discharge pressure, and has to be recompressed in order to achieve a high enough pressure for the gas to be able to exit through the discharge port. This recompression work results in a steep drop in efficiency, since the recompression process is irreversible, more so than the expansion process for this machine, and is a direct reduction on the power produced. This explains why experimental work (e.g. Woodland *et al*, 2012 and Lemort *et al*, 2009) has shown a larger degradation in efficiency for the over-expanded case than the under-expanded case. Therefore, it is advisable to err on the side of under-expansion (fill factor greater than 1) than over-expansion (fill factor less than 1) to achieve better performances at off-design operating conditions.

The comprehensive model also provides a useful tool to gauge the relative influence of specific parameters on the performance of the machine. As an example, Figure 11 illustrates the mass flow rates from the various leakage paths in the spool expander (for the perfectly expanded case). Since the processes in all chambers are periodic about every half rotation (i.e. for each rotation, there are two suction, expansion, and discharge processes), the results for half a rotation are sufficient to characterize the system since the results for the second half would be identical. Note that the gap widths used to calculate the leakage areas were typical of those emanating from sealing and manufacturing considerations. As a reference, the average mass flow rate entering the expander shell over the entire rotation is approximately 4.2 kg/s, with a peak of over 15 kg/s during the suction process.
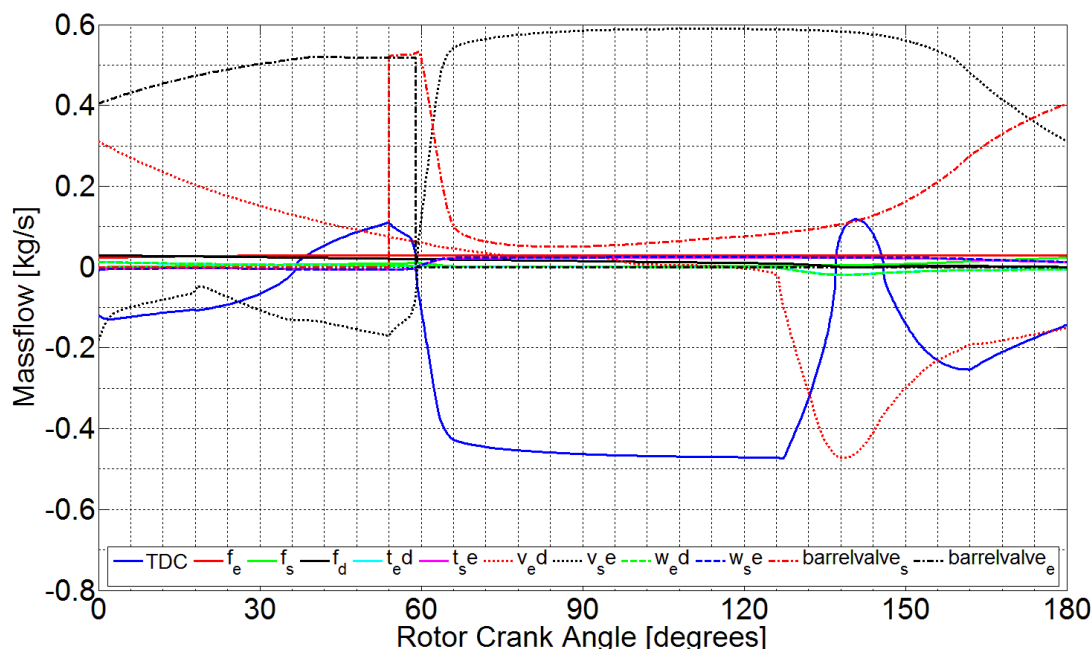
Figure 11: Leakage flow rates for spool expander from various leak paths.

Figure 11 shows that the leakage paths around the suction valve, the vane and the TDC account for a far larger share of the total leakage than other pathways. Therefore, it would be advisable to minimize the clearance between the suction valve and the housing, the vane and the stator surface and/or increase the stator relief rather than expend effort in other parts of the machine to reduce leakage. Similar insights can be provided by the model to assess other design parameters on performance.

4. CONCLUSION

A comprehensive model of the spool expander is presented, which includes submodels for the geometry, suction valve mechanism, massflow, leakage and heat transfer. The resulting mass and energy balances provide the framework to assess the performance of the system. An analysis of Pressure-Volume diagrams reveals that the alignment of the built-in expansion ratio and the system imposed pressure ratio plays an important role in the performance of the expander. Furthermore, the model provides valuable insight into the phenomena behind these results, and shows that from a performance perspective, under-expansion is preferable to over-expansion. The model is also able to discern dominant performance characteristics, for example that leakage around the suction valve, the vane and the TDC account for by far the largest leakage paths. Similar insights can be obtained to assess the sensitivity of various design variables on expander performance. In future work, the model predictions will be validated using experimental data from a 50kW prototype spool expander. The results and experience derived from test system will be used to refine the model and provide a more complete understanding of expander technology.

NOMENCLATURE

D_h	Hydraulic diameter	(m)
f	Face seal leak path	(-)
h	Enthalpy	(kJ kg^{-1})
h_c	Convective heat transfer coefficient	(W/m^2·K)
k	Thermal Conductivity	(W/m·K)
$\dot{m}$	Mass flow	(kg s^{-1})
$\dot{m}_{in}$	Mass flow in	(kg s^{-1})
$\dot{m}_{out}$	Mass flow out	(kg s^{-1})
Pr	Prandtl number	(-)

$\dot{Q}$	Heat transfer rate	(W)
Re	Reynolds number	(-)
r	radius	(m)
T	Temperature	(K)
t	tip leak path	(-)
TDC	Top Dead Center	(-)
u	Internal energy	(kJ kg^{-1})
V	Volume	(m^3)
v	vane leak path	(-)
w	wrap around leak path	(-)

Greek Symbols

θ	Rotor crank angle	(radians)
ρ	Density	(kg m^{-3})
ω	Rotational speed	(rad s^{-1})

Subscript

s	suction
e	expansion
d	discharge

REFERENCES

Bell, I. (2011). Theoretical and experimental analysis of liquid flooded compression in scroll compressors. *PhD thesis*, Purdue University.

Bradshaw, C. R., & Groll, E. A. (2013). A comprehensive model of a novel rotating spool compressor. *International Journal of Refrigeration*, *36*(7), 1974-1981.

Kemp, G. T., Garrett, N., & Groll, E. A. (2008). Novel rotary spool compressor design and preliminary prototype performance. In *Proceedings of the 19th International Compressor Engineering Conference at Purdue University*.

Lemort, V., Quoilin, S., Cuevas, C., & Lebrun, J. (2009). Testing and modeling a scroll expander integrated into an Organic Rankine Cycle. *Applied Thermal Engineering*, *29*(14), 3094-3102.

Mathison, M. M., Braun, J. E., & Groll, E. A. (2008). Modeling of a two-stage rotary compressor. *HVAC&R Research*, *14*(5), 719-748.

Mathison, M. M., Braun, J. E., & Groll, E. A. (2012). Modeling of a Novel Spool Compressor with Multiple Injection Ports. *PhD thesis*, Purdue University.

Norton, R. L. (2009). *Cam design and manufacturing handbook*. Industrial Press Inc. ISBN-13: 9780831133672.

Woodland, B. J., Braun, J. E., Groll, E. A., & Horton, W. T. (2012). Experimental testing of an organic Rankine cycle with Scroll-type expander. In *Proceedings of the 2010 International Refrigeration and Air Conditioning Conference,* Purdue University, 2505.